Journal of Orthopaedic Surgery and Research

RESEARCH

Open Access

Parthenolide ameliorates glucocorticoid-induced inhibition of osteogenic differentiation and osteoporosis by activating ERK signaling pathway

Yanling Feng[1*] and Zhaoyang Li[2]

Abstract

Background Parthenolide (PTL) is a natural sesquiterpene lactone that possesses significant effects on stimulating osteoblast differentiation. The present study focused on the potential of PTL in the treatment of glucocorticoid-induced osteoporosis (GIOP).

Methods MC3T3-E1 cells were treated with dexamethasone (DEX; 10 μM) or/and PTL (5, 10, and 20 μM). The changes in osteogenic differentiation were analyzed by conducting ALP and Alizarin Red staining and assessing the levels of osteogenic markers (Runx2, Osx, and OPN). PTL (3 and 10 mg/kg/day) was injected into rat models of GIOP induced by DEX. Bone formation was analyzed by assessing the levels of bone turnover markers (ALP, TRAP, OCN, and CTx) in the serum and osteoblast differentiation markers (BMP2 and Runx2) in the femurs. The pathological changes of the femurs were determined by H&E staining. Bone mass and osteoblast numbers in the femurs were measured. Western blotting evaluated ERK phosphorylation in vitro and in vivo.

Results PTL promoted osteogenic differentiation and enhanced the levels of Runx2, Osx, OPN, and ERK phosphorylation in DEX-treated MC3T3-E1 cells. ERK inhibitor U0126 reversed the promoting effect of PTL on osteogenesis in DEX-treated MC3T3-E1 cells. After the administration of PTL in rat models of GIOP, the levels of ALP, TRAP, OCN, and CTx in the serum and the levels of BMP2, Runx2, and ERK phosphorylation in the femurs were restored. PTL increased trabecular bone number, reduced trabecular separation, and increased the number of osteoblasts in GIOP rat model.

Conclusion Overall, PTL alleviates osteoporosis by promoting osteogenic differentiation via activation of ERK signaling.

Keywords Parthenolide, Osteoporosis, Glucocorticoid, Bone formation, ERK

*Correspondence:
Yanling Feng
18093192897@163.com
[1]Department of Endocrinology and Metabolism, The Second Hospital of Lanzhou University, No.82, Cuiyingmen, Lanzhou 730030, Gansu Province, China
[2]The Second Clinical Medical School, Lanzhou University, Lanzhou 730000, China

Introduction

Osteoporosis is an age- and sex-specific disease, and one in three women and one in five men over the age of 50 will experience an osteoporotic fracture [1–3]. Glucocorticoids [4] are widely used to alleviate various inflammatory conditions and treat lymphoproliferative diseases and other systemic diseases [5]. However, there is a rapid phase of bone loss and increased risk of bone fractures in most of the post-menopausal women and older men that orally receive GC [6, 7]. High GC levels have been reported to suppress osteoblast differentiation and function, leading to the suppression of bone formation; long-term GC treatment may cause glucocorticoid-induced osteoporosis (GIOP) [8]. GIOP is a clinically common cause of secondary osteoporosis, and the increasing disability rate caused by GIOP has imposed a huge burden on society worldwide [9, 10]. The currently available treatment for osteoporosis includes selective estrogen receptor modulation, hormone replacement therapy, as well as anti-osteoporotic drugs such as zoledronic acid and bisphosphonates, immunosuppressants, and corticosteroids [11]. However, all these therapies have limitations as they cause serious side effects [12]. Thus, it is needed to identify effective therapeutic approaches that can mitigate the development of GIOP.

In recent decades, many active ingredients of traditional Chinese medicine have been favored owning to their beneficial effects on the prevention of GIOP with few side effects [13–16]. *Tanacetum vulgare* L. is a type of traditional Chinese herbal medicine, which is commonly used to quell fevers, treat migraines, and alleviate joint pains [17]. Parthenolide (PTL) is a small sesquiterpenoid molecule extracted from the aerial parts of *Tanacetum vulgare* L [18]. PTL has been revealed to exhibit widely potent biological activities including anticancer [19], antinociceptive [20], antifibrotic [21], antioxidant [22], anti-inflammatory [23], neuroprotective [24], and cardioprotective actions [25]. Moreover, studies have demonstrated the role of PTL in bone homeostasis. For example, PTL was shown to inhibit osteoclastic bone resorption [26, 27]. Zhang et al. revealed its promoting effect on osteoblast differentiation under inflammatory conditions via Wnt/β-Catenin signaling [28]. In addition, its protective effect against cartilage damage and osteoclastogenesis in rheumatoid arthritis has been reported [29, 30]. Researchers also highlighted the inhibitory effect of PTL on surface bone loss during calvarial osteolysis [31]. More importantly, the anti-osteoporosis activity of PTL has been reported, which demonstrates that it exerts anti-apoptotic action in H_2O_2-treated osteoblasts [32]. However, the specific function and underlying mechanism of PTL in GIOP remain to be fully understood.

In this study, the antiosteoporosis effect of PTL was investigated in MC3T3-E1 cells stimulated by dexamethasone (DEX, a synthetic glucocorticoid) and GIOP rat models. Furthermore, the possible signaling pathway involved was investigated.

Materials and methods

Cell culture and treatment

MC3T3-E1 cells were purchased from the Cell Bank of the Chinese Academy of Sciences (Shanghai, China) and cultured in alpha minimum essential medium (α-MEM; HyClone, UT, USA) containing 10% FBS (foetal bovine serum; HyClone) at 37 °C in a 5% CO_2 incubator. For cell differentiation, the medium was replaced by osteogenic medium (OM) supplemented with α-MEM, FBS (10%), ascorbic acid (50 μg/mL; Sigma-Aldrich, MO, USA), and glycerophosphate (10 Mm; Sigma-Aldrich). To investigate the effect of PTL on osteoblastic differentiation, MC3T3-E1 cells were cultured in OM with DEX (10 μM; Cat. No. D1756; Sigma-Aldrich) or/and PTL for different periods of time (7 and 14 days). PTL (purity of 98%; Cat. No. wkq-00599) was purchased from Sichuan Weikeqi Biological Technology Co., Ltd. (Chengdu, Sichuan, China) and added to the culture 12 h before stimulation with DEX. This is the first study to investigate the effect of PTL on MC3T3-E1 osteoblasts. Therefore, we used a gradient of increasing concentration of PTL (0-200 μM) to select the optimum concentration of PTL. To conduct the signaling experiments, extracellular signal-regulated kinase (ERK) inhibitor U0126 (10 μM; Cat. No. M00009; Biolab, Beijing, China) was added 1 h before PTL treatment. The concentration of U0126 was selected according to previous reports [33, 34].

Cell counting Kit-8 (CCK-8) assay

MC3T3-E1 cells (1×10^3 cells/well) were incubated in 96-well plates overnight and treated with PTL at different concentrations (1, 5, 10, 20, 50, 100, and 200 μM) for 48 h to assess the cytotoxicity. To evaluate the changes in cell viability, MC3T3-E1 cells were treated with DEX (10 μM) and PTL (5, 10, and 20 μM). Then, the CCK-8 solution (10 μL; Beyotime, Shanghai) was added for 2 h of incubation at 37 °C, and the absorbance was measured using a microplate reader (Qiagen, Germany) at the wavelength of 450 nm.

Alkaline phosphatase (ALP) staining

MC3T3-E1 cells were seeded in 6-well plates at a density of 1×10^5 cells/well and incubated in OM for 7 days. Then, cells were treated with BCIP/NBT ALP Color Development Kit (Beyotime) following the manufacturer's instruction. The excess dye was rinsed off with water, and a light microscope (Nikon, Tokyo, Japan) was used to observe the staining results. ALP activity was detected using ALP Assay Kit (Sigma-Aldrich) according to the standard protocol.

Alizarin red staining

MC3T3-E1 cells were seeded in 6-well plates (2×10^5 cells per well) and osteogenesis was determined at 14 days in OM. After fixation in 4% paraformaldehyde (Beyotime) for 30 min, cells were stained with 0.2% Alizarin Red solution (Sigma-Aldrich) for 30 min. To quantify mineralization nodules, calcium deposits were desorbed using 10% cetylpyridinium chloride (Sigma-Aldrich) for 30 min, and the absorbance at 562 nm was measured using a microplate reader.

Reverse transcription quantitative real-time polymerase chain reaction (RT-qPCR)

Total RNA was extracted from the treated MC3T3-E1 cells using TRIzol reagent (Takara, Dalian, China) and then reverse-transcribed into cDNA using RevertAid First Strand cDNA Synthesis Kit (Thermo Fisher Scientific, MA, USA). 2×SYBR Green qPCR MasterMix (Biolab) was used to perform RT-qPCR in ABI Prism 7900 (Applied Biosystems; Thermo Fisher Scientific). The expression levels of for runt-related transcription factor 2 (Runx2), osterix (Osx), and osteopontin (OPN) were calculated using the standard $2^{-\Delta\Delta CT}$ method. β-actin mRNA was used as internal control. The primer sequences of the genes analyzed in the present study are listed in Table 1.

Animal model

SD rats (female; ~230 g; 6–8 weeks old) from Medical Experimental Center in Lanzhou University were housed in standard environment. All the rats were randomly divided into four groups ($n = 10$ in each group): control; DEX; DEX + 3 mg/kg PTL; DEX + 10 mg/kg PTL. To establish the GIOP model, the rats were subcutaneously injected with DEX at a dose of 1.5 mg/kg for 6 weeks (3 times/week) as previously described [35]. The rats in the PTL-treated groups were intraperitoneally injected with 3 mg/kg/day or 10 mg/kg/day PTL for 2 weeks before DEX treatment and the drug administration continued for another 6 weeks. The doses of PTL were determined according to previous report [26]. The rats in the control group received 0.9% saline. After 6 or 8 weeks of PTL administration, all the rats were euthanized by CO_2 inhalation. Blood samples (2 mL) were collected from the inferior vena cava, and left femurs were isolated for western and histopathological analysis. All animal procedures were carried out in accordance with the principles of the Ethics Committee of The Second Hospital of Lanzhou University (No. D2025-356).

Determination of ALP, tartrate-resistant acid phosphatase (TRAP), osteocalcin (OCN), and C-terminal telopeptide of type I collagen (CTx) in serum

After 8 weeks of PTL administration, the blood samples were collected and centrifuged at 3000×g for 20 min at 4 °C. Then, the serum levels of ALP, TRAP, OCN, and CTx were determined using ALP Assay Kit (Sigma-Aldrich), TRAP Assay Kit (Nanjing Jiancheng, Nanjing, China), OCN Assay Kit, and CTx Assay Kit (USCN, Wuhan, China), respectively, according to the manufacturer's instruction.

Western blotting

MC3T3-E1 cells and femurs from the rats were lysed in an ice-cold RIPA buffer (Beyotime), and then the homogenates were centrifuged at 12,000×g for 10 min at 4 °C. To determine the protein concentration, BCA Protein Assay Kit (Beyotime) was used. The protein was separated by 10% SDS-PAGE and transferred to PVDF membranes (Millipore, MA, USA). After blocking in 5% skimmed milk for 1 h, anti-Runx2 (ab236639; 1:1000), anti-Osx (ab209484; 1:1000), anti-OPN (ab283656; 1:1000), anti-P-ERK (ab201015; 1:1000), anti-ERK (ab184699; 1:10000), anti-bone morphogenetic protein 2 (BMP2) (ab284387; 1:1000), and anti-β-actin (ab6276; 1:5000) primary antibodies were incubated with the membranes overnight at 4 °C. The primary antibodies used above were provided by Abcam (MA, USA). Then, the membranes were incubated with HRP-labeled secondary antibody (1:500; Beyotime) for 2 h at room temperature. Finally, the blots were detected by enhanced chemiluminescence (ECL) reagent (Beyotime). β-actin was used as loading control. Protein bands were quantified using Image Lab Software version 6.1 (Bio-Rad, CA, USA).

Hematoxylin and eosin (H&E) staining

After 6 or 8 weeks of PTL administration, all the rats were euthanized. The femurs were fixed in neutral buffered formalin (10%), paraffin-embedded, and then cut into 6-μm-thick sections. After the gradient dehydration and rehydration, the sections were stained with hematoxylin and eosin (Solarbio, Beijing), and then the stained sections were observed by light microscopy. Bone morphometric parameters including trabecular area (Tb.

Table 1 The primers used in this manuscript

GENE	Forward primer	Reverse primer
Runx2	GAATGCACTACCCAGCCAC	TGGCAGGTACGTGTGGTAG
Osx	AGGAGGCACAAAGAAGCCATAC	AGGGAAGGGTGGGTAGTCATT
OPN	TCCAAAGCCAGCCTGGAAC	TGACCTCAGAAGATGAACTC
β-actin	GCCAACCGTGAAAAGATGAC	ACCAGAGGCATACAGGGACAG

Ar), trabecular number (Tb.N), trabecular separation (Tb. Sp), and osteoblast number/bone surface (N.ob/BS) were analyzed using Image-Pro Plus Software version 6.0 (Media Cybernetics, Inc., MD, USA).

Statistical analysis

SPSS 23.0 software (SPSS, Inc., Chicago, IL, USA) was used for data analysis. Results were expressed as mean ± standard deviation. One-way ANOVA followed by Tukey's *post hoc* test was performed to assess differences among groups. The difference was considered statistically significant when the *p* value was less than 0.05.

Results

PTL accelerates osteogenic differentiation of MC3T3-E1 cells

After 48 h of incubation with PTL at different concentrations, MC3T3-E1 cells treated with PTL concentration more than 20 μM exhibited significantly reduced viability (Fig. 1A). DEX stimulation impaired cell viability in MC3T3-E1 cells. However, the viability was not restored after incubation with 5, 10, and 20 μM of PTL (Fig. 1B). We further detected the effect of PTL (10 and 20 μM) on osteogenic differentiation of MC3T3-E1 cells. According to the results of ALP staining and activity, DEX reduced

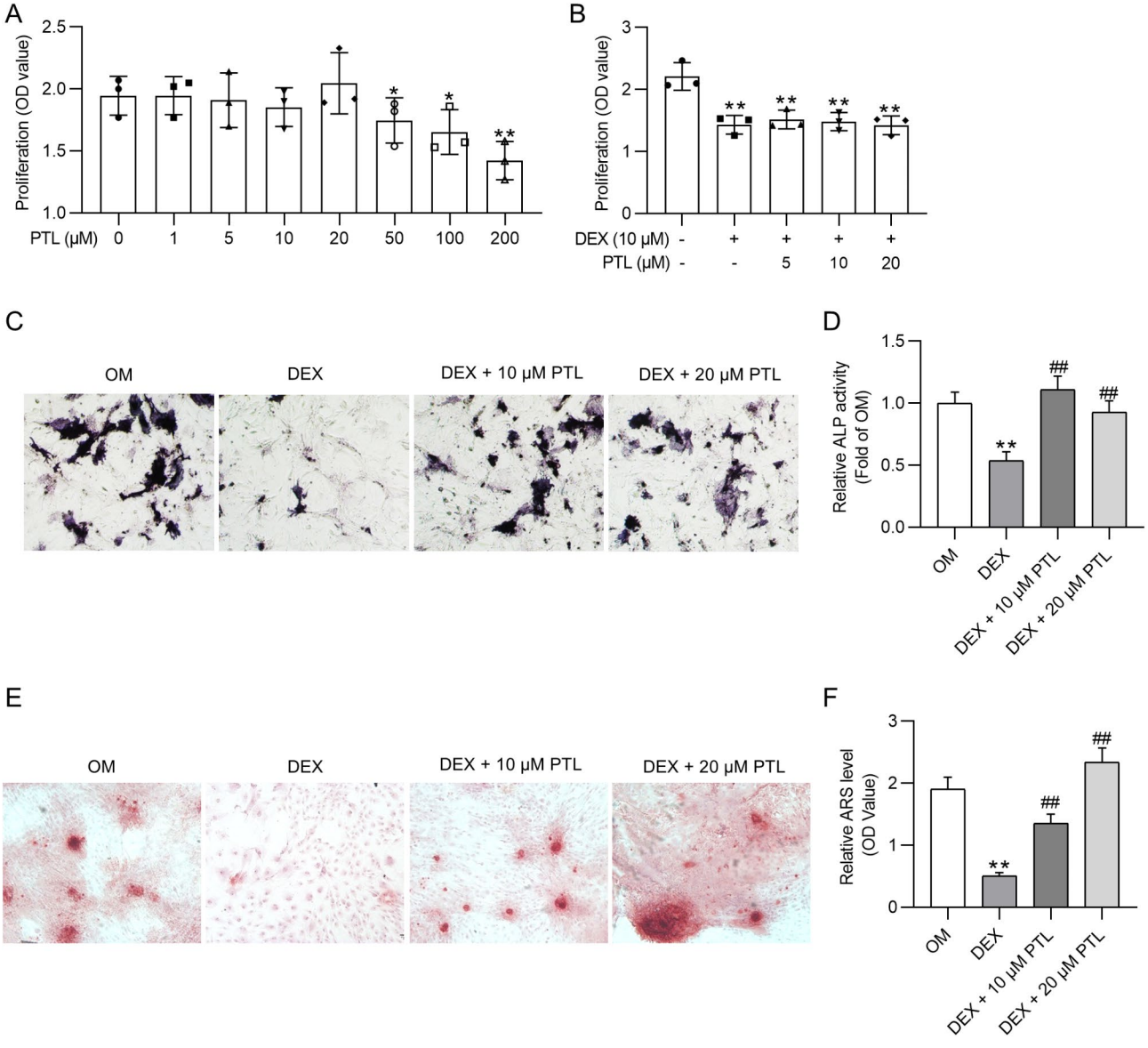

Fig. 1 PTL regulates bone formation and bone resorption in GIOP rat model. (**A**) Serum levels of ALP, (**B**) TRAP, (**C**) OCN, (**D**) and CTx in GIOP rats were evaluated by corresponding detection kits. (**E-F**) Western blotting of BMP2 and Runx2 protein levels in the femurs. (**G-H**) Western blotting of ERK phosphorylation in the femurs. $N = 10$. $^{**}p < 0.01$ vs. control group; $^{\#}p < 0.05$, $^{\#\#}p < 0.01$ vs. DEX group. PTL, parthenolide; DEX, dexamethasone; ALP, alkaline phosphatase; TRAP, tartrate-resistant acid phosphatase; OCN, osteocalcin; CTx, C-terminal telopeptide of type I collagen; GIOP, glucocorticoid-induced osteoporosis; BMP2, bone morphogenetic protein 2; Runx2, runt-related transcription factor 2; ERK, extracellular signal-regulated kinase

osteogenic potential of MC3T3-E1 cells, and the reduction was markedly reversed by 10 and 20 μM of PTL treatment (Fig. 1C and D). Alizarin Red staining also showed that PTL increased staining density and mineralized nodules in MC3T3-E1 cells stimulated with DEX (Fig. 1E and F).

PTL promotes osteogenesis and activates ERK signaling in DEX-treated MC3T3-E1 cells

To further confirm the effect of PTL on MC3T3-E1 osteoblast differentiation, the expression of several osteoblast markers was evaluated after 7 days of incubation. Runx2, Osx, and OPN mRNA expression levels were significantly reduced by DEX stimulation and restored by PTL treatment (Fig. 2A and C).

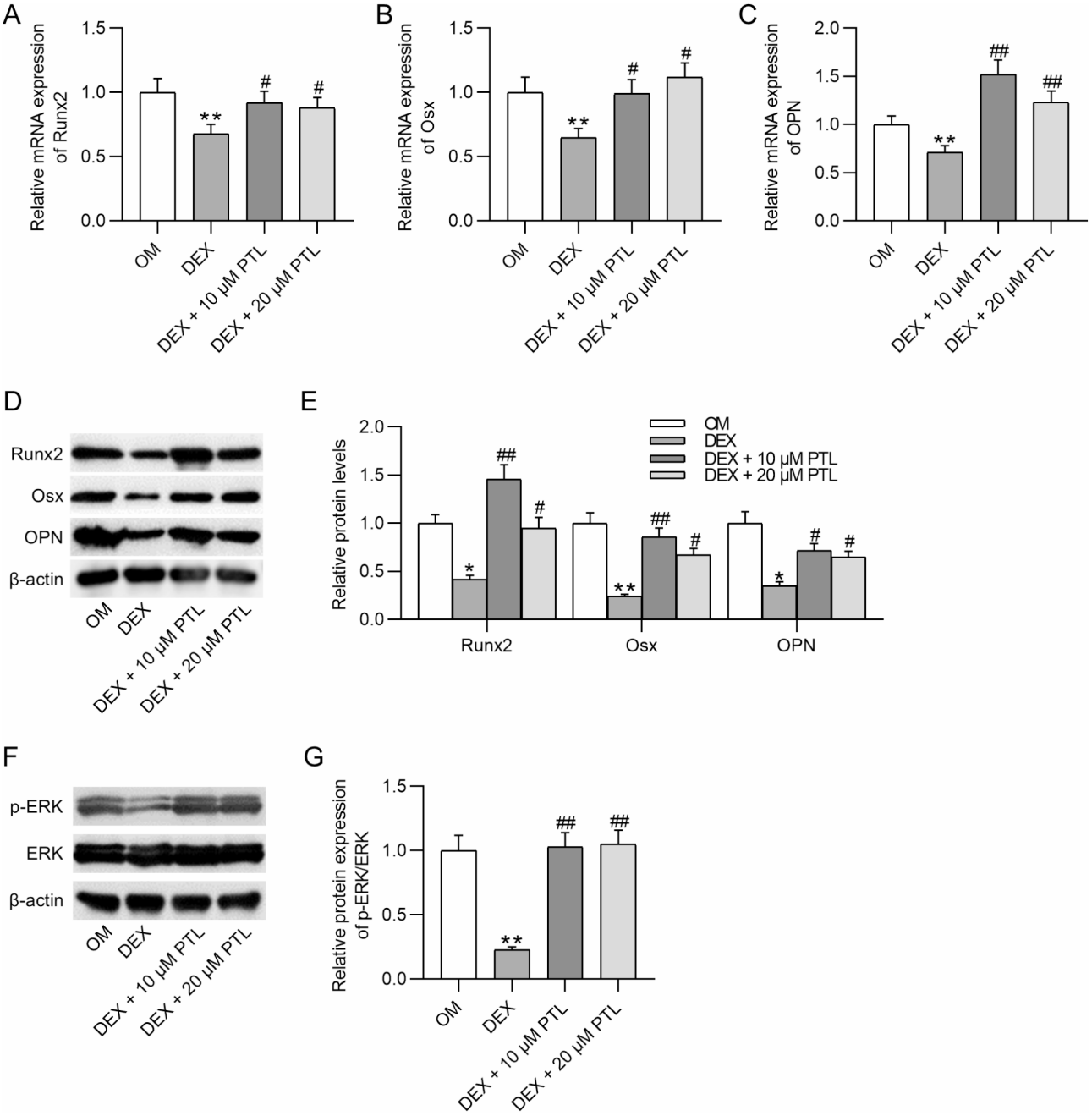

Fig. 2 PTL promotes osteogenesis and activates ERK signaling in DEX-treated MC3T3-E1 cells. RT-qPCR analysis of (**A**) Runx2, (**B**) Osx, and (**C**) OPN mRNA expression, and (**D-E**) western blotting of the levels of Runx2, Osx, and OPN proteins and (**F-G**) ERK phosphorylation in MC3T3-E1 cells treated with DEX and PTL for 7 days. $N = 3$. $^{*}p < 0.05$, $^{**}p < 0.01$ vs. OM group; $^{\#}p < 0.05$, $^{\#\#}p < 0.01$ vs. DEX group. PTL, parthenolide; DEX, dexamethasone; OM, osteogenic medium; Runx2, runt-related transcription factor 2; Osx, osterix; OPN, osteopontin; ERK, extracellular signal-regulated kinase

The reduced protein levels of Runx2, Osx, and OPN induced by DEX in MC3T3-E1 cells were significantly rescued by PTL (Fig. 2D and E). Many studies have shown that ERK signaling pathway activates Runx2 and is involved in regulating osteoblast differentiation [36, 37]. We thus investigated the participation of ERK signaling. Obviously, the levels of phosphorylated ERK protein were decreased after DEX stimulation. However, treatment with PTL promoted the phosphorylation of ERK protein (Fig. 2F and G).

PTL accelerates osteogenic differentiation of MC3T3-E1 cells by activating ERK signaling

MC3T3-E1 cells were pretreated with U0126 (ERK inhibitor; 10 μM) to detect whether ERK signaling participates in the effect of PTL on osteogenesis. Western blotting showed that U0126 significantly abolished the promoting effect of PTL on the protein levels of phosphorylated ERK in DEX-treated MC3T3-E1 cells (Fig. 3A and B). The increased ALP staining and activity induced by PTL treatment in DEX-treated MC3T3-E1 cells were also reversed by U0126 (Fig. 3C and D). Consistently, the effect of PTL on Alizarin Red staining density and mineralized nodules was counteracted by U0126 (Fig. 3E and F).

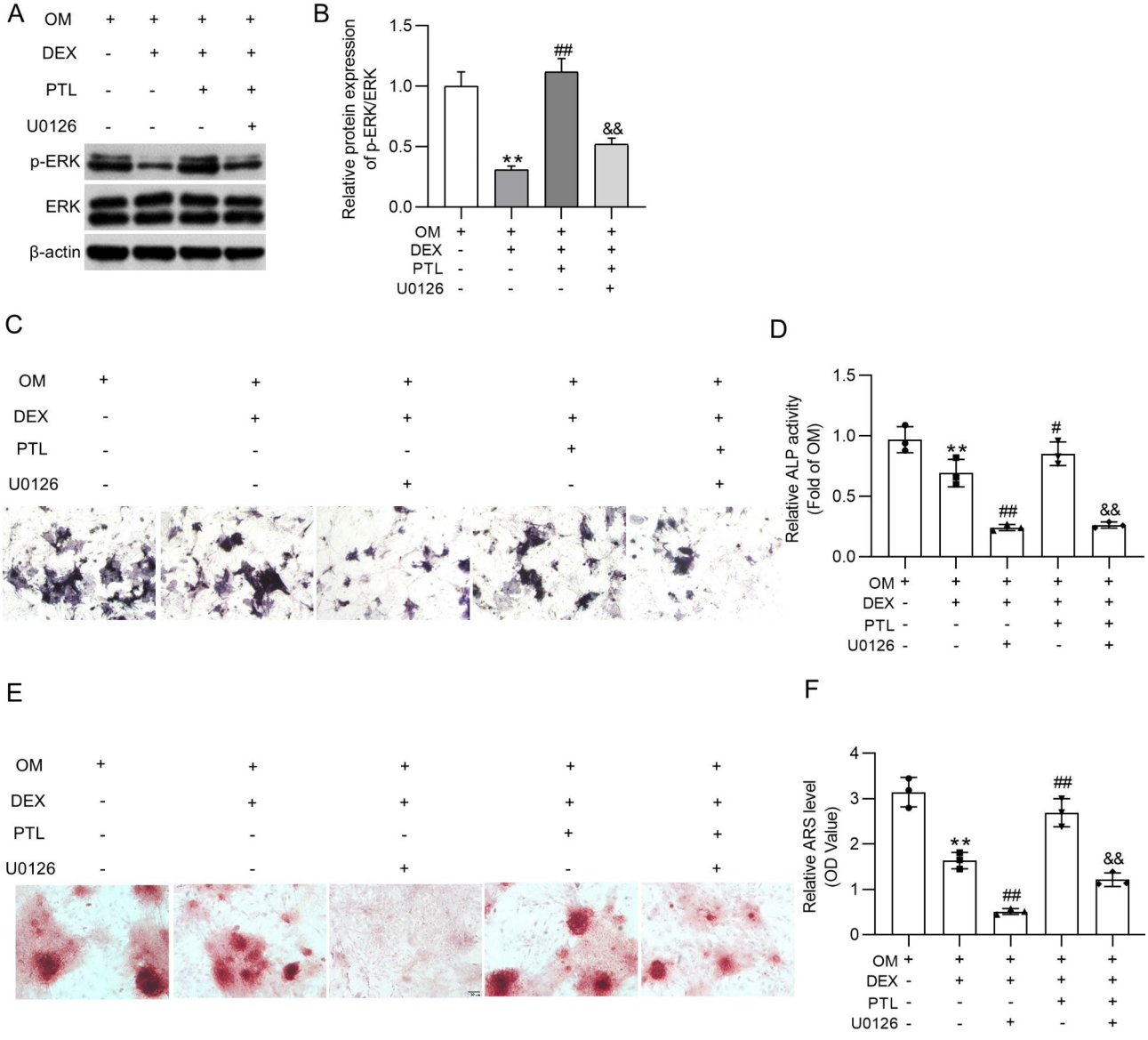

Fig. 3 PTL accelerates osteogenic differentiation of MC3T3-E1 cells by activating ERK signaling. (**A-B**) Western blotting assessed the levels of ERK phosphorylation in MC3T3-E1 cells treated with DEX, PTL, and U0126. (**C-D**) ALP staining and (**E-F**) Alizarin Red staining in MC3T3-E1 cells treated with DEX, PTL, and U0126. $N = 3$. $^{**}p < 0.01$ vs. OM group; $^{\#}p < 0.05$, $^{\#\#}p < 0.01$ vs. DEX group; $^{\&\&}p < 0.01$ vs. PTL group. PTL, parthenolide; DEX, dexamethasone; ALP, alkaline phosphatase; OM, osteogenic medium; ERK, extracellular signal-regulated kinase

PTL regulates bone formation and bone resorption in GIOP rat model

After 8 weeks of PTL administration, blood samples were collected to evaluate the effect of PTL on bone turnover markers in serum. Compared with the control group, DEX-treated rats showed decreased serum levels of bone formation markers (ALP and OCN) and increased serum levels of bone resorption-related markers (TRAP and CTx), while GIOP rats with PTL treatment exhibited upregulated ALP and OCN levels and downregulated TRAP and CTx levels in serum (Fig. 4A and D). Moreover, the protein levels of osteoblast markers (BMP2 and Runx2) were reduced in the GIOP rat model group and were restored by PTL treatment (Fig. 4E and F). We further confirmed the effect of PTL on ERK phosphorylation in vivo. The results showed that ERK phosphorylation was inhibited in the GIOP group compared with the control group. Treatment with PTL significantly restored the phosphorylation of ERK protein in vivo (Fig. 4G and H).

PTL increases bone mass and the number of osteoblasts in GIOP rat model

H&E staining was performed in the proximal femurs to assess histological changes. After 4 weeks of PTL administration, there were no statistically significant differences in trabecular bone microstructure between the DEX group and the DEX + PTL group (data not shown). After 6 or 8 weeks of PTL administration, the GIOP model group displayed a marked deterioration in histological properties compared with those in the control group, including reduced trabecular area and trabecular bone number, as well as increased trabecular separation (Fig. 5A and D). Administration of the PTL to the GIOP model group improved bone parameters and increased osteoblast numbers (Fig. 5A and E). These results suggest that the therapeutic efficacy of PTL is time-dependent, requiring at least 6 weeks of treatment to manifest significant improvements in GIOP.

Discussion

GIOP is induced by long-term overuse of glucocorticoids, which is closely associated with inhibition of bone formation and acceleration of bone resorption [38]. PTL has been shown to inhibit osteoclast differentiation induced by RANKL and promote osteoblast differentiation in inflammatory conditions [27, 28]. In this study, we found that PTL promoted osteogenesis in MC3T3-E1 cells and GIOP animal models induced by DEX via activation of ERK signaling.

Osteoblast differentiation is essential for bone formation [39, 40]. DEX is a commonly used glucocorticoid, and previous studies have shown that DEX exposure inhibits osteoblast proliferation, differentiation, and bone formation [41–44]. Consistently, DEX stimulation suppressed MC3T3-E1 cell viability in our study. We detected the effect of PTL on osteogenesis in DEX-stimulated MC3T3-E1 cells. ALP activity is one of the indicators of osteogenic differentiation, and the process of bone formation is accompanied by the accumulation of matrix mineralization [45]. As expected, DEX stimulation led to suppressed ALP activity and reduced cell mineralization nodules in MC3T3-E1 cells. Interestingly, PTL markedly PTL restored osteogenic differentiation inhibited by DEX. It was noted that the staining density and calcified nodules in the 20 μM PTL group were significantly higher than in the OM group. There could be following reasons: (1) PTL may counteract the inhibitory effect of DEX through multiple mechanisms, such as through activating key signaling pathways that promote osteogenic differentiation and upregulating genes involved in osteogenesis, further enhancing osteogenic differentiation; (2) PTL may have improved cell metabolism or microenvironment, providing more favorable conditions for osteogenic differentiation; (3) The dose or treatment time of PTL may have reached the optimum, so that its pro-differentiation effect is significantly enhanced. The specific mechanism needs further experimental verification. These issues need to be addressed through further research. Runx2 is a osteoblast lineage-determining transcription factor, which plays a critical role in regulating the differentiation of osteoblasts [46]. Runx2 has been shown to induce the expression of various osteogenesis-related markers including Osx, OPN, and OCN [47, 48]. Osx is another important osteoblast-specific transcription factor, and Osx knockout mice exhibit suppressed bone formation [49]. OPN is a multifunctional protein, which is mainly expressed in early osteoblasts [50]. OCN is a well-known downstream osteoblastic gene of Osx and a late differentiation marker [51]. In our study, PTL treatment restored the expression levels of Runx2, Osx, and OPN in DEX-treated MC3T3-E1 cells, which further verified the promoting effect of PTL on osteoblast differentiation.

ERK belongs to the MAPK family and has been demonstrated to participate in regulating the proliferation, differentiation, and mineralization of osteoblasts [52, 53]. During the activation of ERK signaling, phosphorylated ERK modulates osteogenesis by inducing multiple osteogenic transcription regulators such as Runx-2 and Osx [54]. The effect of PTL on ERK signaling has been reported. Kim et al. showed that PTL inhibits RANKL-mediated phosphorylation of ERK in bone marrow macrophages [27]. Zhang et al. reported that PTL exerts anti-osteoclastogenic activity by decreasing ERK activation in human periodontal ligament-derived cells [55]. A previous study revealed the promoting effect of PTL on ERK signaling activation [56]. Here, PTL treatment elevated the levels of phosphorylated ERK protein inhibited by DEX in MC3T3-E1 cells. Moreover, ERK inhibitor

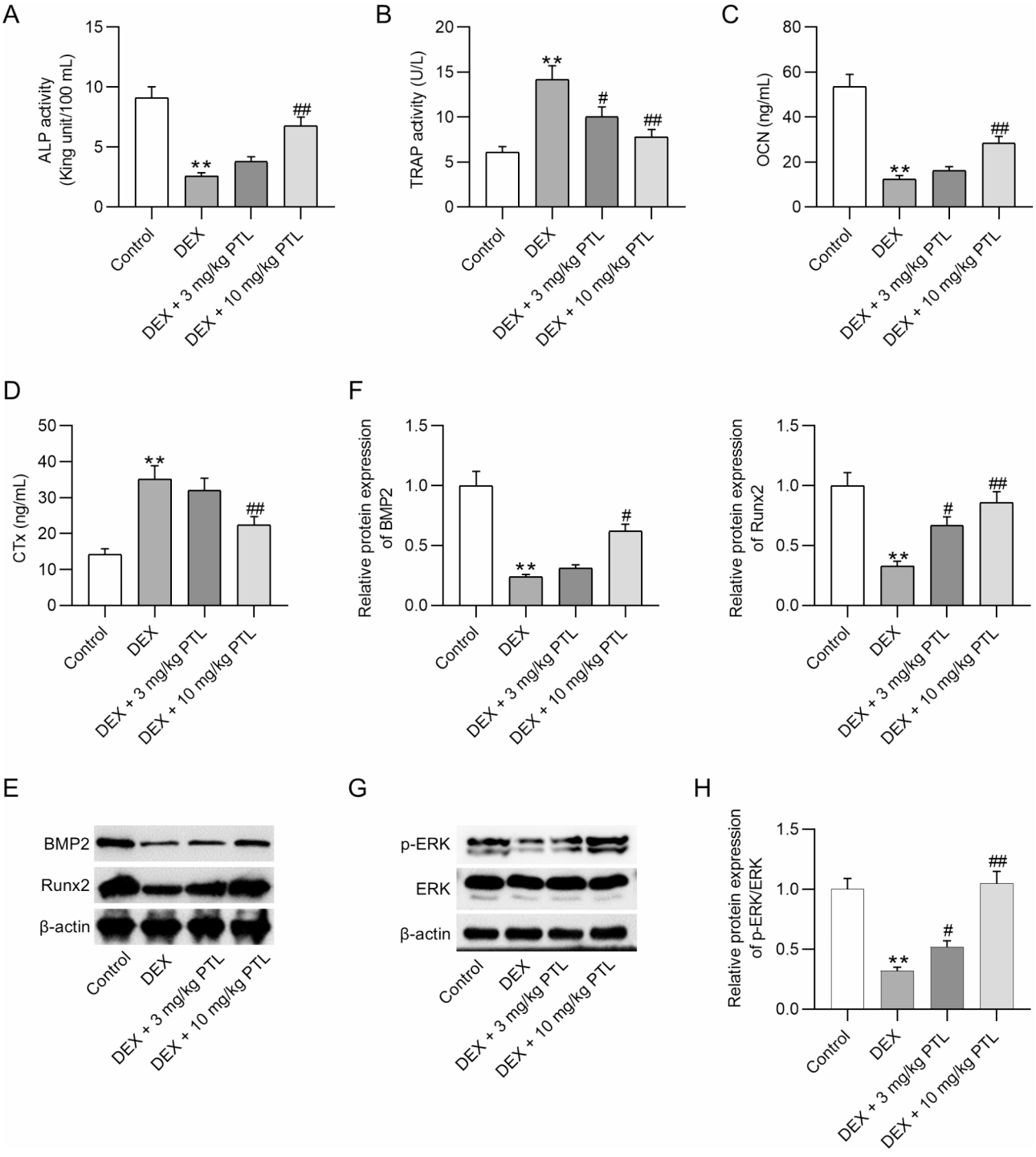

Fig. 4 PTL accelerates osteogenic differentiation of MC3T3-E1 cells. (**A**) CCK-8 assay evaluated the viability of MC3T3-E1 cells after treatment with PTL. (**B**) CCK-8 assay showed the viability of MC3T3-E1 cells after treatment with DEX and PTL. (**C-D**) ALP staining (7 days) and (**E-F**) Alizarin Red staining (14 days) in MC3T3-E1 cells treated with DEX and PTL. $N = 3$. $^{*}p < 0.05$, $^{**}p < 0.01$ vs. control or OM group; $^{\#\#}p < 0.01$ vs. DEX group. PTL, parthenolide; DEX, dexamethasone; ALP, alkaline phosphatase; OM, osteogenic medium

U0126 abolished the promoting effect of PTL on matrix mineralization and ALP activity, which suggested that PTL accelerates osteogenic differentiation of MC3T3-E1 cells in an ERK-dependent manner. Moreover, PTL administration also increased ERK phosphorylation in GIOP rat model.

Bone turnover markers (BTMs) highlight the dynamic balance of the bone tissue. Bone ALP has been considered

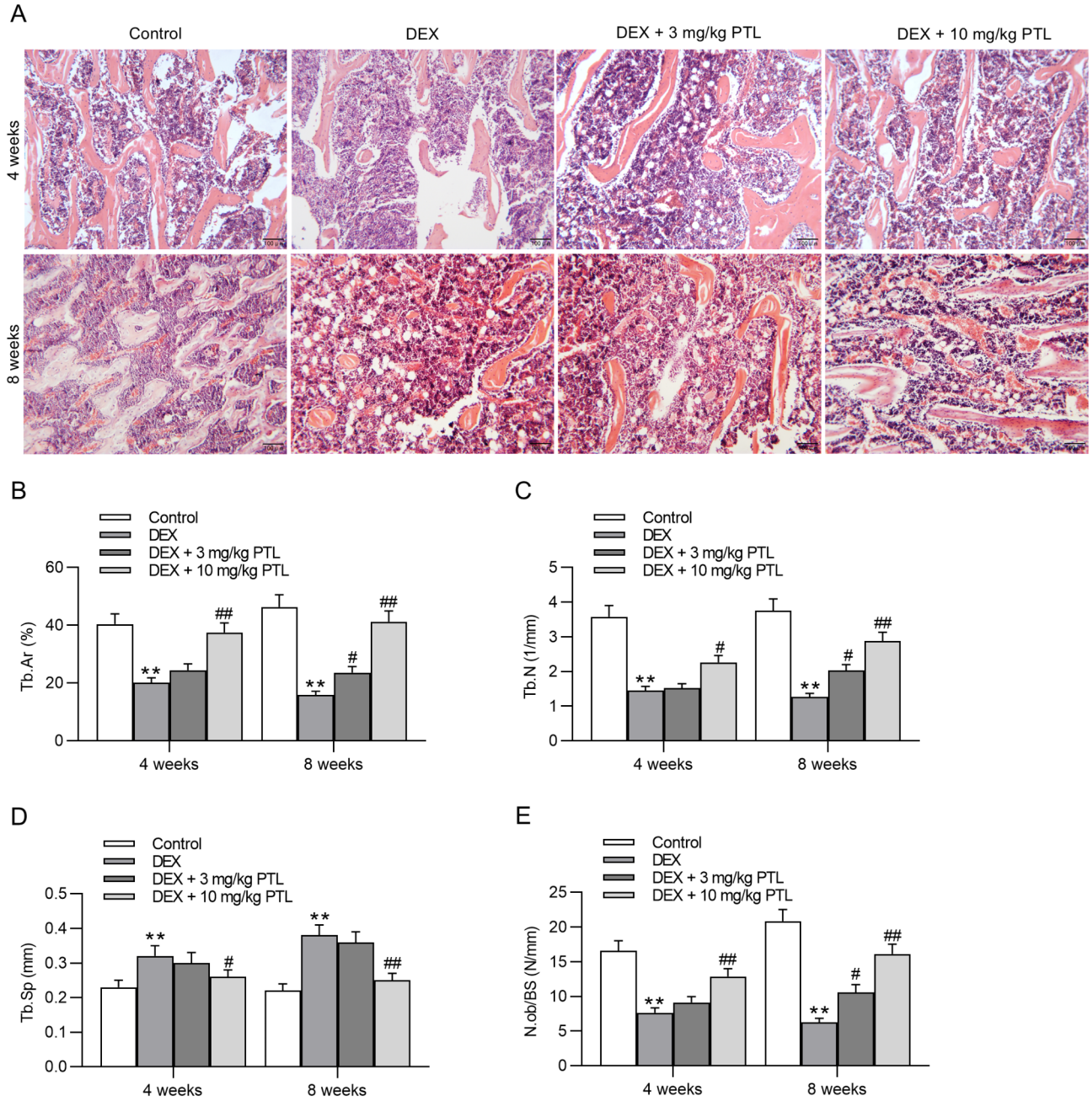

Fig. 5 PTL increases bone mass and the number of osteoblasts in GIOP rat model. (**A**) H&E staining of the proximal femurs. Calculation of bone morphometric parameters including (**B**) Tb.Ar, (**C**) Tb.N, (**D**) Tb.Sp, and (**E**) N.ob/BS in the femurs. $N = 10$. $^{**}p < 0.01$ vs. control group; $^{\#}p < 0.05$, $^{\#\#}p < 0.01$ vs. DEX group. PTL, parthenolide; DEX, dexamethasone; GIOP, glucocorticoid-induced osteoporosis; Tb.Ar, trabecular area ratio; Tb.N, trabecular bone number; Tb.Sp, trabecular separation; N.ob/BS, osteoblast number/bone surface

biomarker of bone ossification, while serum CTx is an indicator of bone resorption [57, 58]. TRAP is an enzyme marker for osteoclasts [59]. In the serum of DEX-induced GIOP rats, ALP and OCN levels were decreased. Meanwhile, the serum levels of TRAP and CTx were elevated. Interestingly, PTL treatment in GIOP rats remarkably rescued the levels of these indicators, suggesting its effect on promoting bone formation and suppressing bone resorption. BMP2 is a fundamental component of the inherent regenerative capacity of bone [60]. Runx2 can be activated by BMP2, and their interaction is essential for osteoblast differentiation [61]. Here, we further observed enhanced BMP2 and Runx2 expression levels in PTL-treated GIOP rat model. More importantly, PTL increased trabecular bone number, reduced trabecular separation, and increased the number of osteoblasts

in GIOP rat model. All these results suggested that PTL accelerates bone formation to alleviate GIOP in vivo.

There are still some limitations in our study. First, we only focused on the effect of PTL on osteogenesis and ERK signaling, and its influence on other pathways or factors involved in GIOP, such as Epidermal Growth Factor (EGF) signaling [62], other pathways associated with bone formation, and RANK/RANKL/OPG pathway related to osteoclastogenesis [63], remain to be investigated. Second, the in vivo study focused on a rat GIOP model, which may not fully recapitulate the pathophysiology of GIOP in humans. Additionally, the study lacks clinical relevance. Human samples, such as bone marrow-derived mesenchymal stem cells from patients with GIOP, should be used to further verify our findings in the future.

In conclusion, our findings highlight that PTL alleviates osteoporosis induced by glucocorticoid by accelerating osteoblast differentiation and mineralization. In addition, the effect of PTL on osteogenesis is associated with the activation of ERK signaling pathway. The results of this study expand the application of PTL and provide a basic investigation for the therapy of GIOP.

Acknowledgements
We appreciate all participants who contributed to the study.

Author contributions
Yanling Feng conceived and designed the experiments. Yanling Feng and Zhaoyang Li carried out the experiments. Yanling Feng and Zhaoyang Li analyzed the data. Yanling Feng drafted the manuscript. All authors agreed to be accountable for all aspects of the work. All authors have read and approved the final manuscript.

Funding
This study was funded by Cuiying Scientific Training Program for Undergraduates of The Second Hospital of Lanzhou University (CYXZ2022-11) and National College Students' Innovation and Entrepreneurship Training Program (20241703).

Data availability
All data generated or analyzed during the current study are available from the corresponding author on reasonable request.

Declarations

Ethics approval
All animal procedures were carried out in accordance with the principles of the Ethics Committee of The Second Hospital of Lanzhou University (No. D2025-356).

Competing interests
The authors declare no competing interests.

Received: 14 January 2025 / Accepted: 15 March 2025
Published online: 09 May 2025

References

1. Andersen M, Andresen AK, Hartvigsen J, Hermann AP, Sørensen J, Carreon LY. Vertebroplasty for painful osteoporotic vertebral compression fractures: a protocol for a single-center doubled-blind randomized sham-controlled clinical trial. VOPE2. J Orthop Surg Res. 2024;19(1):813.
2. Shen L, Yang H, Zhou F, Jiang T, Jiang Z. Risk factors of short-term residual low back pain after PKP for the first thoracolumbar osteoporotic vertebral compression fracture. J Orthop Surg Res. 2024;19(1):792.
3. Leeyaphan J, Rojjananukulpong K, Intarasompun P, Peerakul Y. Simple clinical predictors for making directive decisions in osteoporosis screening for women: a cross-sectional study. J Orthop Surg Res. 2024;19(1):789.
4. Misra S, Bagchi A, Sarkar A, Niyogi S, Bhattacharjee D, Chatterjee S, Mondal S, Chattopadhyay A, Saha A, Chatterjee S, et al. Methotrexate and theaflavin-3, 3'-digallate synergistically restore the balance between apoptosis and autophagy in synovial fibroblast of RA: an ex vivo approach with cultured human RA FLS. Inflammopharmacology. 2021;29(5):1427–42.
5. Oray M, Abu Samra K, Ebrahimiadib N, Meese H, Foster CS. Long-term side effects of glucocorticoids. Exp Opin Drug Saf. 2016;15(4):457–65.
6. Migliorini F, Giorgino R, Hildebrand F, Spiezia F, Peretti GM, Alessandri-Bonetti M, Eschweiler J, Maffulli N. Fragility fractures: risk factors and management in the elderly. Med (Kaunas Lithuania). 2021;57(10):1119.
7. Migliorini F, Colarossi G, Eschweiler J, Oliva F, Driessen A, Maffulli N. Antiresorptive treatments for corticosteroid-induced osteoporosis: a bayesian network meta-analysis. Br Med Bull. 2022;143(1):46–56.
8. Conti V, Russomanno G, Corbi G, Toro G, Simeon V, Filippelli W, Ferrara N, Grimaldi M, D'Argenio V, Maffulli N, et al. A polymorphism at the translation start site of the vitamin D receptor gene is associated with the response to anti-osteoporotic therapy in postmenopausal women from Southern Italy. Int J Mol Sci. 2015;16(3):5452–66.
9. Migliorini F, Maffulli N, Colarossi G, Eschweiler J, Tingart M, Betsch M. Effect of drugs on bone mineral density in postmenopausal osteoporosis: a bayesian network meta-analysis. J Orthop Surg Res. 2021;16(1):533.
10. Bao X, Liu C, Liu H, Wang Y, Xue P, Li Y. Association between polymorphisms of glucagon-like peptide-1 receptor gene and susceptibility to osteoporosis in Chinese postmenopausal women. J Orthop Surg Res. 2024;19(1):869.
11. Migliorini F, Colarossi G, Baroncini A, Eschweiler J, Tingart M, Maffulli N. Pharmacological management of postmenopausal osteoporosis: a level I evidence Based - Expert opinion. Expert Rev Clin Pharmacol. 2021;14(1):105–19.
12. Lei C, Song JH, Li S, Zhu YN, Liu MY, Wan MC, Mu Z, Tay FR, Niu LN. Advances in materials-based therapeutic strategies against osteoporosis. Biomaterials. 2023;296:122066.
13. Chen Z, Xue J, Shen T, Mu S, Fu Q. Curcumin alleviates glucocorticoid-induced osteoporosis through the regulation of the Wnt signaling pathway. Int J Mol Med. 2016;37(2):329–38.
14. Zhao Y, Wang HL, Li TT, Yang F, Tzeng CM. Baicalin Ameliorates Dexamethasone-Induced Osteoporosis by Regulation of the RANK/RANKL/OPG Signaling Pathway. Drug design, development and therapy. 2020;14:195–206.
15. Xie B, Wu J, Li Y, Wu X, Zeng Z, Zhou C, Xu D, Wu L. Geniposide alleviates Glucocorticoid-Induced Inhibition of osteogenic differentiation in MC3T3-E1 cells by ERK pathway. Front Pharmacol. 2019;10:411.
16. Huang F, Wang Y, Liu J, Cheng Y, Zhang X, Jiang H. Asperuloside alleviates osteoporosis by promoting autophagy and regulating Nrf2 activation. J Orthop Surg Res. 2024;19(1):855.
17. Onozato T, Nakamura CV, Cortez DA, Dias Filho BP, Ueda-Nakamura T. Tanacetum vulgare: antiherpes virus activity of crude extract and the purified compound parthenolide. Phytother Res. 2009;23(6):791–6.
18. Freund RRA, Gobrecht P, Fischer D, Arndt HD. Advances in chemistry and bioactivity of parthenolide. Nat Prod Rep. 2020;37(4):541–65.
19. Sztiller-Sikorska M, Czyz M. Parthenolide as cooperating agent for Anti-Cancer treatment of various malignancies. Pharmaceuticals (Basel Switzerland). 2020;13(8):194.
20. Materazzi S, Benemei S, Fusi C, Gualdani R, De Siena G, Vastani N, Andersson DA, Trevisan G, Moncelli MR, Wei X, et al. Parthenolide inhibits nociception and neurogenic vasodilatation in the trigeminovascular system by targeting the TRPA1 channel. Pain. 2013;154(12):2750–58.
21. Zhang Y, Huang Q, Chen Y, Peng X, Wang Y, Li S, Wu J, Luo C, Gong W, Yin B, et al. Parthenolide, an NF-κB inhibitor, alleviates peritoneal fibrosis by suppressing the TGF-β/Smad pathway. Int Immunopharmacol. 2020;78:106064.
22. Wang JA, Tong ML, Zhao B, Zhu G, Xi DH, Yang JP. Parthenolide ameliorates intracerebral hemorrhage-induced brain injury in rats. Phytother Res. 2020;34(1):153–60.
23. Liu YJ, Tang B, Wang FC, Tang L, Lei YY, Luo Y, Huang SJ, Yang M, Wu LY, Wang W, et al. Parthenolide ameliorates colon inflammation through regulating Treg/Th17 balance in a gut microbiota-dependent manner. Theranostics. 2020;10(12):5225–41.
24. Ding W, Cai C, Zhu X, Wang J, Jiang Q. Parthenolide ameliorates neurological deficits and neuroinflammation in mice with traumatic brain injury by

suppressing STAT3/NF-κB and inflammasome activation. Int Immunopharmacol. 2022;108:108913.
25. Skoumal R, Tóth M, Serpi R, Rysä J, Leskinen H, Ulvila J, Saiho T, Aro J, Ruskoaho H, Szokodi I, et al. Parthenolide inhibits STAT3 signaling and attenuates angiotensin II-induced left ventricular hypertrophy via modulation of fibroblast activity. J Mol Cell Cardiol. 2011;50(4):634–41.
26. Idris AI, Krishnan M, Simic P, Landao-Bassonga E, Mollat P, Vukicevic S, Ralston SH. Small molecule inhibitors of IkappaB kinase signaling inhibit osteoclast formation in vitro and prevent ovariectomy-induced bone loss in vivo. FASEB Journal: Official Publication Federation Am Soc Experimental Biology. 2010;24(11):4545–55.
27. Kim JY, Cheon YH, Yoon KH, Lee MS, Oh J. Parthenolide inhibits osteoclast differentiation and bone resorbing activity by down-regulation of NFATc1 induction and c-Fos stability, during RANKL-mediated osteoclastogenesis. BMB Rep. 2014;47(8):451–6.
28. Zhang X, Chen Q, Liu J, Fan C, Wei Q, Chen Z, Mao X. Parthenolide promotes differentiation of osteoblasts through the Wnt/β-Catenin signaling pathway in inflammatory environments. J Interferon Cytokine Research: Official J Int Soc Interferon Cytokine Res. 2017;37(9):406–14.
29. Liu Q, Zhao J, Tan R, Zhou H, Lin Z, Zheng M, Romas E, Xu J, Sims NA. Parthenolide inhibits pro-inflammatory cytokine production and exhibits protective effects on progression of collagen-induced arthritis in a rat model. Scand J Rheumatol. 2015;44(3):182–91.
30. Williams B, Lees F, Tsangari H, Hutchinson MR, Perilli E, Crotti TN. Assessing the effects of parthenolide on inflammation, bone loss, and glial cells within a collagen Antibody-Induced arthritis mouse model. Mediat Inflamm. 2020;2020:6245798.
31. Zawawi MS, Marino V, Perilli E, Cantley MD, Xu J, Purdue PE, Dharmapatni AA, Haynes DR, Crotti TN. Parthenolide reduces empty lacunae and osteoclastic bone surface resorption induced by polyethylene particles in a murine calvarial model of peri-implant osteolysis. J Biomedical Mater Res Part A. 2015;103(11):3572–9.
32. Mao W, Zhu Z. Parthenolide inhibits hydrogen peroxide–induced osteoblast apoptosis. Mol Med Rep. 2018;17(6):8369–76.
33. Fan S, Gao X, Chen P, Li X. Myricetin ameliorates glucocorticoid-induced osteoporosis through the ERK signaling pathway. Life Sci. 2018;207:205–11.
34. Gu Q, Chen M, Zhang Y, Huang Y, Yang H, Shi Q. Haem oxygenase-1 induction prevents glucocorticoid-induced osteoblast apoptosis through activation of extracellular signal-regulated kinase1/2 signalling pathway. J Orthop Translation. 2019;19:29–37.
35. Hozayen WG, El-Desouky MA, Soliman HA, Ahmed RR, Khaliefa AK. Antiosteoporotic effect of petroselinum crispum, ocimum Basilicum and cichorium intybus L. in glucocorticoid-induced osteoporosis in rats. BMC Complement Altern Med. 2016;16:165.
36. Jaiswal RK, Jaiswal N, Bruder SP, Mbalaviele G, Marshak DR, Pittenger MF. Adult human mesenchymal stem cell differentiation to the osteogenic or adipogenic lineage is regulated by mitogen-activated protein kinase. J Biol Chem. 2000;275(13):9645–52.
37. Lai CF, Chaudhary L, Fausto A, Halstead LR, Ory DS, Avioli LV, Cheng SL. Erk is essential for growth, differentiation, integrin expression, and cell function in human osteoblastic cells. J Biol Chem. 2001;276(17):14443–50.
38. Henneicke H, Gasparini SJ, Brennan-Speranza TC, Zhou H, Seibel MJ. Glucocorticoids and bone: local effects and systemic implications. Trends Endocrinol Metab. 2014;25(4):197–211.
39. Barnaba S, Papalia R, Ruzzini L, Sgambato A, Maffulli N, Denaro V. Effect of pulsed electromagnetic fields on human osteoblast cultures. Physiotherapy Res International: J Researchers Clin Phys Therapy. 2013;18(2):109–14.
40. Giai Via A, McCarthy MB, de Girolamo L, Ragni E, Oliva F, Maffulli N. Making them commit: strategies to influence phenotypic differentiation in mesenchymal stem cells. Sports Med Arthrosc Rev. 2018;26(2):64–9.
41. Wang N, Wang H, Chen J, Wang F, Wang S, Zhou Q, Ying J, Huang S, Wang P, Yuan F. ACY–1215, a HDAC6 inhibitor, decreases the dexamethasone–induced suppression of osteogenesis in MC3T3–E1 cells. Mol Med Rep. 2020;22(3):2451–59.
42. Feng YL, Tang XL.Effect of glucocorticoid-induced oxidative stress on the expression of Cbfa1. Chem Biol Interact. 2014;25:207:26–31.
43. Takahashi M, Ushijima K, Hayashi Y, Maekawa T, Ando H, Tsuruoka S, Fujimura A. Dosing-time dependent effect of dexamethasone on bone density in rats. Life Sci. 2010;86(1–2):24–9.
44. Liu Y, Cui Y, Chen Y, Gao X, Su Y, Cui L. Effects of dexamethasone, celecoxib, and methotrexate on the histology and metabolism of bone tissue in healthy Sprague Dawley rats. Clin Interv Aging. 2015;10:1245–53.
45. Hoemann CD, El-Gabalawy H, McKee MD. In vitro osteogenesis assays: influence of the primary cell source on alkaline phosphatase activity and mineralization. Pathol Biol. 2009;57(4):318–23.
46. Wysokinski D, Pawlowska E, Blasiak J. RUNX2: A master bone growth regulator that May be involved in the DNA damage response. DNA Cell Biol. 2015;34(5):305–15.
47. Sinha KM, Zhou X. Genetic and molecular control of Osterix in skeletal formation. J Cell Biochem. 2013;114(5):975–84.
48. Yao KL, Todescan R Jr., Sodek J. Temporal changes in matrix protein synthesis and mRNA expression during mineralized tissue formation by adult rat bone marrow cells in culture. J Bone Mineral Research: Official J Am Soc Bone Mineral Res. 1994;9(2):231–40.
49. Nakashima K, Zhou X, Kunkel G, Zhang Z, Deng JM, Behringer RR, de Crombrugghe B. The novel zinc finger-containing transcription factor Osterix is required for osteoblast differentiation and bone formation. Cell. 2002;108(1):17–29.
50. Nakamura A, Dohi Y, Akahane M, Ohgushi H, Nakajima H, Funaoka H, Takakura Y. Osteocalcin secretion as an early marker of in vitro osteogenic differentiation of rat mesenchymal stem cells. Tissue Eng Part C Methods. 2009;15(2):169–80.
51. Gu H, Boonanantanasarn K, Kang M, Kim I, Woo KM, Ryoo HM, Baek JH. Morinda citrifolia leaf extract enhances osteogenic differentiation through activation of Wnt/β-Catenin signaling. J Med Food. 2018;21(1):57–69.
52. Wanachewin O, Boonmaleerat K, Pothacharoen P, Reutrakul V, Kongtawelert P. Sesamin stimulates osteoblast differentiation through p38 and ERK1/2 MAPK signaling pathways. BMC Complement Altern Med. 2012;12:71.
53. Jeong HM, Han EH, Jin YH, Hwang YP, Kim HG, Park BH, Kim JY, Chung YC, Lee KY, Jeong HG. Saponins from the roots of platycodon grandiflorum stimulate osteoblast differentiation via p38 MAPK- and ERK-dependent RUNX2 activation. Food Chem Toxicology: Int J Published Br Industrial Biol Res Association. 2010;48(12):3362–8.
54. Miraoui H, Oudina K, Petite H, Tanimoto Y, Moriyama K, Marie PJ. Fibroblast growth factor receptor 2 promotes osteogenic differentiation in mesenchymal cells via ERK1/2 and protein kinase C signaling. J Biol Chem. 2009;284(8):4897–904.
55. Zhang X, Fan C, Xiao Y, Mao XJE. -bc, eCAM am. Anti-inflammatory and anti-osteoclastogenic activities of parthenolide on human periodontal ligament cells in vitro. 2014;2014:546097.
56. D'Anneo A, Carlisi D, Lauricella M, Emanuele S, Di Fiore R, Vento R. Tesoriere GJJocp. Parthenolide induces caspase-independent and AIF-mediated cell death in human osteosarcoma and melanoma cells. 2013;228(5):952–67.
57. Migliorini F, Maffulli N, Spiezia F, Tingart M, Maria PG, Riccardo G. Biomarkers as therapy monitoring for postmenopausal osteoporosis: a systematic review. J Orthop Surg Res. 2021;16(1):318.
58. Migliorini F, Maffulli N, Spiezia F, Peretti GM, Tingart M, Giorgino R. Potential of biomarkers during Pharmacological therapy setting for postmenopausal osteoporosis: a systematic review. J Orthop Surg Res. 2021;16(1):351.
59. Lee YJ, Ahn JC, Oh CH. Oxyresveratrol attenuates bone resorption by inhibiting the mitogen-activated protein kinase pathway in ovariectomized rats. Nutr Metabolism. 2024;21(1):7.
60. Kay AG, Dale TP, Akram KM, Mohan P, Hampson K, Maffulli N, Spiteri MA, El Haj AJ, Forsyth NR. BMP2 repression and optimized culture conditions promote human bone marrow-derived mesenchymal stem cell isolation. Regen Med. 2015;10(2):109–25.
61. Phimphilai M, Zhao Z, Boules H, Roca H, Franceschi RT. BMP signaling is required for RUNX2-dependent induction of the osteoblast phenotype. J Bone Mineral Research: Official J Am Soc Bone Mineral Res. 2006;21(4):637–46.
62. Mangiavini L, Peretti GM, Canciani B, Maffulli N. Epidermal growth factor signalling pathway in endochondral ossification: an evidence-based narrative review. Ann Med. 2022;54(1):37–50.
63. Udagawa N, Koide M, Nakamura M, Nakamichi Y, Yamashita T, Uehara S, Kobayashi Y, Furuya Y, Yasuda H, Fukuda C, et al. Osteoclast differentiation by RANKL and OPG signaling pathways. J Bone Miner Metab. 2021;39(1):19–26.

Publisher's note